Polymer(Korea), Vol. 30, No. 3, pp 187-195, 2006

초청논문

유기 저항막을 이용한 원자힘 현미경 양극산화 패터닝 기술

김성경 · 이해원[†]

한양대학교

Anodic Oxidation Lithography via Atomic Force Microscope on Organic Resist Layers

Sung-Kyoung Kim and Haiwon Lee[†]

Department of Chemistry, Hanyang University, Seoul 133-791, Korea

초록 : 원자힘 현미경 양극산화 패터닝 기술에 관한 연구를 유기 저항막의 종류 및 그들의 특성을 토대로 다루었다. 본 연구실에서 수행한 자기조립막, 랑뮈어-블라짓막, 고분자막 위에서의 원자힘 현미경 양극산화 패터닝에 대한 연구결과를 중심으로, 유기 저항막 위에서의 원자힘 현미경 양극산화 패터닝 기술에 대한 이해를 돕고자 하였다. 현실적인 공정 속도에서 높은 종횡비의 패턴을 형성하기 위해 원자힘 현미경 양극산화 패터닝에 유기 저항막의 전기-기계적 특성, 젖음 특성, 에칭 저항 특성 등이 중요한 인자들임을 제안하였다.

Abstract : Atomic force microscope (AFM)-based anodic oxidation lithography has gained great interests in fabricating nanometer scale features on semiconductor or metal substrates beyond the limitation of optical lithography. In this article AFM anodic oxidation lithography and its organic resist layers are introduced based on our previous works. Organic resist layers of self-assembled monolayers, Langmuir-Blodgett films and polymer films are suggested to play a key role in enhancing the aspect ratio of producing features, the lithographic speed, and spatial precision in AFM anodic oxidation lithography.

Keywords : atomic force microscope, nanolithography, anodic oxidation or anodization, organic resist, self-assembled monolayer, Langmuir-Blodgett film, polymer resist.

Content

1. Introduction 187
2. Anodization Lithography on Organic Resist Layers 188
 2.1 Introduction of AFM Anodization Lithography
 2.2 Site-Selective Assembly on a Protruded Oxide Feature
 2.3 Local Oxidation on Organic Resist Layers
3. Summary 194
4. References 194

Introduction

Since the invention of the scanning probe microscope (scanning tunneling microscope, STM[1] and atomic force microscope, AFM[2]), it has been one of the most widely used instruments in nanoscience and nanotechnology. Due to the use of their tip with a small curvature (usually < 20 nm), it is possible to image or create nanometer-scale features on desired substrates. In the industry especially of semiconductor or electronics, a great challenge for engineering structures in sub-100 nanometer scale has been performed to overcome the limitations in optical lithography for the last tens of years.[3,4] Recently, scanning probe lithography (SPL) was considered as an alternative to realizing the sub-100 nanometer feature-sized devices with a fraction of the cost of optical and e-beam techniques.[5-9] The SPL has been applied to various potential researches for the modification of substrates with a large variety of techniques. However, substantial development still remains to be used for patterning large areas in manufacturing. This article introduces our efforts to evolve the nanotechnology related to the fabrication of patterns with nanometer-scale feature size using SPL. Scanning tunneling microscopy (STM) and atomic force microscopy (AFM) are mainly included in SPL that consists of using the tip as an electro-mechanical tool on various material surfaces. The SPL is commonly used in the local change of

†To whom correspondence should be addressed.
E-mail: haiwon@hanyang.ac.kr

any properties of surface by a scanning probe microscope tip. The most striking example for the local change was found in the precise positioning of individual atoms of xenon[10] and silicon[11] with an STM tip. Nanodroplets of an ink(e.g. 16-mercaptohexadecanoic acid) were written with nm-scale resolution onto a substrate using an AFM tip, called dip-pen nanolithography.[4,12] Adsorbate molecules like self-assembled monolayers(SAMs) were patterned under a high local pressure of an AFM tip, called nanoshaving.[6] Besides these examples above, the variety of lithography applications using organic monolayers and thin films were conducted with the patterning mechanisms ranging from electron-activated processes using conducting tips to thermomechanical indentation using an AFM tip.[13-18] One of the most promising SPLs has been considered as the anodic oxidation which involves the direct modification of the surface(semiconductor or metal) and use of organic materials as lithographically active layers.[19-41] In which, a biased tip selectively oxidizes a surface to fabricate nanometer scale oxide patterns in the process of anodic oxidation lithography(or called anodization lithography). In the case, many factors influence reproducibility, lateral resolution, writing speed, and etc. Organic resist layers provide an attractive option for anodization SPL, as well as for other SPLs. In the view point of chemistry, organic thin layers provide not only chemical modification of the substrate to introduce new functionalities but also electronically/photonically sensitive layers to chemically modify a material at nanometer scales. In anodization lithography process, electrons are field-emitted from the negatively biased conducting tip to a sample. If a sample is coated with an organic thin layer, the emitted electrons traverse the layer that absorbs energy from the electron radiation, resulting in inducing chemical changes in the organic layer. Moreover, organic resist layers provide many advantages, such as low threshold voltage, high sensitivity, sub-100 nm resolution, good dry etch resistance, and etc. We, here, focus on the anodization SPL on organic resist layers of self-assembled monolayers, Langmuir-Blodgett monolayers and polymers using a biased tip as an electron source.

Anodization Lithography on Organic Resist Layers

Introduction of Atomic-Force Microscope (AFM) Anodization Lithography. The scanning probe lithography(SPL) using scanning tunneling microscope(STM) has shown successful applications in electron exposure of a surface.[19,22] The operation of the STM under tunneling mode, however, has limited its use on an insulating surface, for instance, like a polymer film. In contrast, atomic force microscope(AFM) is operated by optically detecting the deflections of the cantilever due to tip-substrate interatomic forces. Therefore, broad applications were accomplished with AFM-based lithography in the ambient condition.

Some AFM-based nanolithographic methods are not practical since their lithographic speed is only the order of nanometer/second, and both nanografting[23,24] and current sensing AFM lithography[25] are usually accomplished under liquid-solid interface. In this sense, AFM anodization lithography is an excellent solution to fabricating highly resolved nano patterns at the high speed without environmental restrictions. Using the technique, oxide patterns could be protruded on a substrate by faradaic current passing from the cathode tip to the anode substrate.[26-41] Anodic patterning can be mainly performed on silicon or titanium substrate by electrochemical reactions mediated by the scanning probe tip. This direct modification of silicon or metal surfaces by the anodization process using the electric field from an AFM tip is one promising method of accomplishing direct-writing lithography for the electronic device fabrication. Sugimura and co-workers have suggested an electrochemical reaction between the tip and the sample for the anodization lithography as follows :[27]

Anode reactions at sample surface :

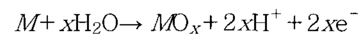

$M + xH_2O \rightarrow MO_x + 2xH^+ + 2xe^-$

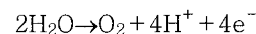

$2H_2O \rightarrow O_2 + 4H^+ + 4e^-$

Cathode reaction at AFM tip:

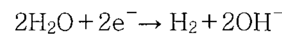

$2H_2O + 2e^- \rightarrow H_2 + 2OH^-$

The first report of tip-induced oxidation of silicon was the STM study by Dagata *et al.* They used an H-passivated silicon surface with a positively biased tip for generating oxide features on the surface.[19] They suggested that the electrochemical oxidation reaction, which is locally induced beneath the tip in an adsorbed water column on the sample surface, is responsible for the modification of metal and semiconductor surfaces. Since the AFM anodization lithography is closely related to the magnitude of current, the size of the protruded pattern strongly depends on the amount of accepted electrons on the substrate. Also, it has been reported that the geometric factors of the nanopattern such as the protruding height and the line-width are affected by scan speed or duration time of the cathode AFM tip,[31,32] surface group,[36,40] environmental relative humidity[29,32,36] and the applied voltage

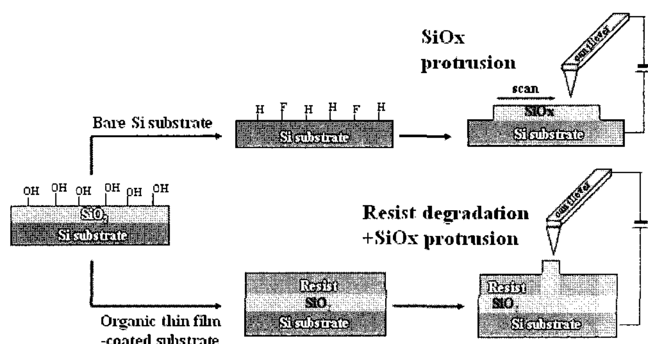

Figure 1. Schematic description of AFM anodization nano-lithography on H-passivated Si and organic thin film-coated Si substrate.

between the tip and the sample.[28,29] Even the operational mode of AFM, both contact mode and non-contact mode also influences on anodization pattering.[41]

Figure 1 shows a simple description of AFM anodization lithography on H-passivated Si substrate and on organic resist-coated Si substrate. In the latter case, the emitted electrons flow from the tip to the substrate through an organic resist, and the degradation of the resist happen due to electron bombardment through the water column. Accordingly, a protruded oxide pattern is newly formed at the local area of the substrate as a result of the anodization process.

The selection of high-performance resist materials is one of the most important factors in the successful application of AFM lithography. In AFM anodization lithography, the conductive tip on a resist emits low-energy electrons with high current density. Compared to conventional electron beam lithography with high energy of 10-100 keV, the reduced electron backscattering in anodization lithography enables achieving higher resolution. The resist, however, should be prepared into a thinner and uniform film because the lower energy electrons have a shorter penetration depth and therefore we can attain high resolution in nanometer scale. Langmuir-Blodgett (LB) films[34,35] and self-assembled monolayers (SAMs)[33,36,38,40] have been used as thin resists and patterned with nanometer precision. These films are well-organized molecular assemblies formed by layer-by-layer deposition via either van der Waals force or covalent bonding. The size of the molecule determines the layer thickness and can be carefully controlled to produce layers of uniform coverage.[42] SAM films, consisting of organosilane, bipolar amphiphiles, and alkanethiol molecules, show a great potential as ultra thin resist films. Such SAM films, formed through the chemisorption on oxide and metal surfaces, have excellent uniformity in molecular order and resistivity to various types of chemical reagents. A number of lithographic works with organic resists have been exclusively carried out with different functional groups to investigate the surface group effect on the anodic oxidation using AFM.

Site-Selective Assembly on a Protruded Oxide Feature.

The application of the oxide feature protruded by AFM anodization lithography could be found in its use as an etching mask or an insulating barrier. The protruded oxide pattern, however, provides a new active site to react on new functionalities. The thin passive resist layer on an oxidizable substrate was used for the preparation of a site-selective assembly of a desired material, such as carbon nanotubes,[43] quantum dot-sized metal particles,[44] etc. After locally oxidizing the silicon under the organic resist, the protruding SiO_2 can be used in a subsequent chemical modification step in order to introduce new functionalities. Based on the chemical reactions of the functionalized single-walled carbon nanotubes (SWNTs) with surfaces, we tried selective attachments of COCl-SWNTs on patterned surfaces by AFM anodization lithography. Figure 2 shows the fabrication process of selectively attached SWNTs on the protruded SiO_2 region and the results. The self-assembled monolayer (SAM) of hexamethyldisilane (HMDS) was used as a resist so that a substrate was covered by methyl groups ($-CH_3$). AFM anodization lithography produced oxide patterns protruded on a Si substrate under

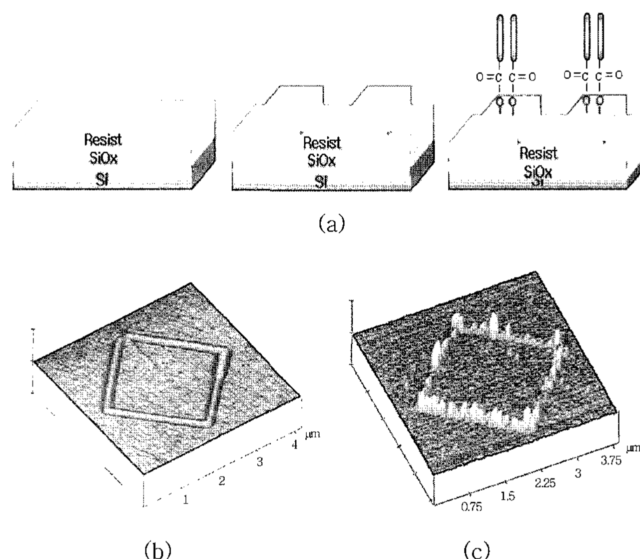

Figure 2. (a) Scheme of the selective attachment of functionalized SWNTs on prepatterned Si surface. (b) Tapping mode AFM image of an oxide pattern on HMDS SAM-passivated Si substrate. (c) Selectively attached SWNTs on the protruded oxide pattern.

HMDS which degrades or oxidizes. The patterned oxide by AFM anodization is covered by –OH groups while the unpatterned area is covered by $-CH_3$ groups. Since there is no reaction between chemically functionalized SWNTs and CH_3 groups, COCl–SWNT can react only on the patterned area containing –OH groups. The similar selective assemblies of not only SWNT but nano–particles were achieved on the various types of patterns.

Local Oxidation on Organic Resist Layers.

AFM Anodization Lithography on Self-Assembled Monolayers : Self–assembled monolayers (SAMs) are very stable because the head group of the self–assembling molecule adsorbs on a substrate with a very strong molecular–substrate interaction, such as covalent bonding or ionic bonding.[42] The self–assembling process was well defined especially for the silanes on hydroxylated surfaces and the thiols on Au surface. The characteristic of the tail group in a self–assembling molecule allow us to modify the surface property, for instance, like hydrophilicity or hydrophobicity. Through previous reports, two kinds of important elements of the tail groups on anodization lithography have been discussed: first, the electrochemical property of the surface functional tail group as an anode surface to affect the lithographyic voltage for the anodization reaction; second, the effect of wetting property of the surface group to water on the width of protruding patterns. Additionally, the sensitivity of SAM resists for anodization lithography depends on the characteristics of the surface groups. To investigate the role of the surface tail group in anodization lithography, we prepared four kinds of SAM resist films with the same alkyl chain (film thickness = ~19 Å) on negatively charged silicon substrate.; *n*–tridecylamine · hydrochloride (TDA · HCl) SAM, 1,12–diaminododecane dihydrochloride (DAD · 2HCl), mixed SAM of TDA · HCl and DAD · 2HCl, and DAD · HCl. Both DAD · 2HCl and TDA · HCl have an ammonium chloride on their headgroups to bind electrostatically onto charged silicon surface. In contrast to the headgroup, they have different tail groups at their air–molecule interfaces. The chemical structures of the molecules are shown in Figure 3.

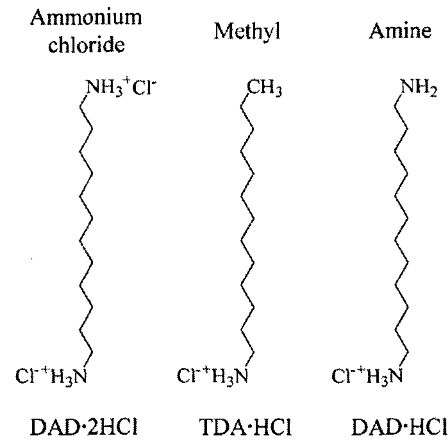

Figure 3. Chemical structures of DAD · 2HCl, TDA · HCl, and DAD · HCl.

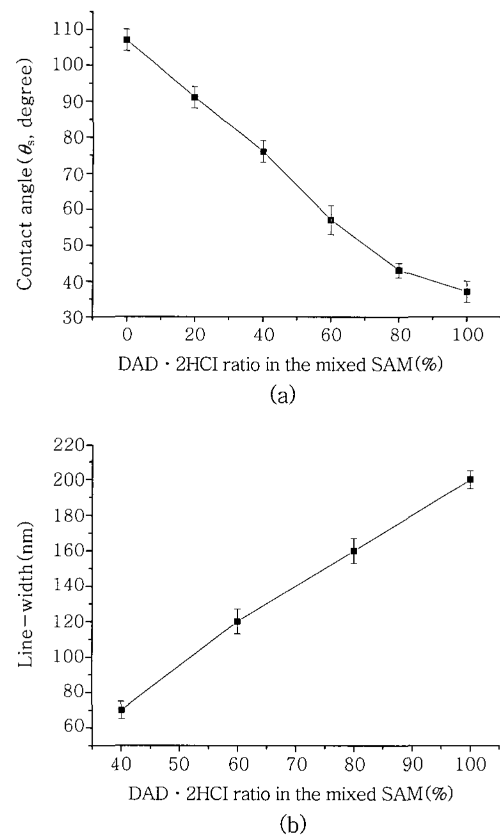

Figure 4. (a) Water contact angle changes and (b) line width changes of the mixed SAMs at the various compositions of DAD · 2HCl and TDA · HCl.

The difference of the mixing ratio of the two molecules had a great influence on wetting property of SAM surface as shown in Figure 4(a). The contact angle for the mixed SAMs decreases dramatically as the amount of the DAD · 2HCl component increases in the monolayer. The ammonium chloride ionic pair, the surface group of DAD · 2HCl, increased the hydrophilicity of the SAM resist, and so enlarged the size of water column between the AFM tip and the substrate interfaces related to the change in contact angle. Figure 4(b) shows that the line width of the protruded pattern increases linearly as the amount of the DAD · 2HCl component in the mixed SAM increases.

Because the newly formed surfaces of SAM resists are prepared on negatively charged substrate and the DAD · 2HCl adsorbate includes ammonium chloride salt as its

Table 1. ξ Potentials and Surface Charge Densities of DAD · 2HCl SAM, D6 Mixed SAM, and TDA · HCl SAM

	1 mM NaCl			10 mM NaCl		
		surface charge density			surface charge density	
	ξ potential (mV)	ions/cm^2	normalized value	ξ potential (mV)	ions/cm^2	normalized value
TDA · HCl · SAM	−1.3	6.00×10^{10}	1	−0.5	6.75×10^{10}	1
D6 mixed SAM	−7.8	3.58×10^{11}	6	−0.8	1.16×10^{11}	2
DAD · 2HCl SAM	−12.9	5.96×10^{11}	10	−1.9	2.69×10^{11}	4
negatively charged surface	−34.9	1.73×10^{12}	29	−20.5	3.05×10^{12}	45

surface group, both the surface potential and the surface charge density are very important for considering the electrostatic characterization of the SAM resist films. The electrical potential at a surface is an important property for obtaining the charge density, which comes from the distribution of the ionic chemical groups at the surfaces of the SAMs. Since the ξ potential allows us to apply the surface potential ψ_s, electrostatic properties of the SAM resists can be examined by measuring the ξ potential. As given in Table 1, for the negatively charged Si wafer surface, the ξ potential was measured as −34.9 and −20.5 mV at 1.0 and 10 mM NaCl concentrations, respectively. We can easily understand the screening effect with the surrounding electrolytes, where the ξ potential increases with decreasing NaCl concentration. From these results the expected ionic charge density on the negatively charged surface by boladication was calculated as 1.73×10^{12} and 3.05×10^{12} ions/cm^2, respectively. The magnitude of ξ potentials of DAD · 2HCl SAM, D6 mixed SAM(mixing ratio of DAD · 2HCl : TDA · HCl=6:4), and TDA · HCl SAM decreases dramatically by the amount of charged ammonium chloride functional group on the surface as −12.9, −7.8, and −1.3 mV in the case of 1 mM NaCl solution, and as −1.9, −0.8, and −0.5 mV in the case of 10 mM NaCl solution, respectively. The estimated surface charge density of molecular films decreases to several tens of times compared to negatively charged surface and the normalized values of the surface charge densities were 1:6:10 in 1.0 mM NaCl solution. These results agreed with the suggested model to fabricate the set of SAM resists: TDA·HCl SAM, D6 mixed SAM, and DAD · 2HCl SAM. The abnormal behavior in 10 mM NaCl solution results from the disturbance of the relatively higher screening effect.[45]

The electron transfer from a tip to a substrate under a tip negative bias can be enhanced by the presence of a functional surface group, especially of positively charged metal ions, on the resist and it affects the lithographic performance. This electron attraction of resist was studied with a functional surface group as an electron acceptor. Various metal phosphate monolayers as resists were prepared on silicon substrates for AFM anodization lithography. The metal phosphate monolayers were formed by binding tetravalent(Zr^{4+}, Hf^{4+}) or divalent(Ca^{2+}, Mg^{2+}) metal ions on a phosphorylated Si substrate. The presence of the metal ions on a phosphorylated Si substrate was confirmed using Auger electron spectroscopy, which shows the electron energies of 142 eV for Zr with the reference value (Ref.) of 151 eV, 1596 eV for Hf with Ref. of 1625 eV, 272 eV for Ca with Ref. of 297 eV, and 1164 eV for Mg with Ref. of 1188 eV. The lithographic results, however, demonstrated the dependence only on the surface charge. The starting voltage of anodization reaction for tetravalent (Zr^{4+}, Hf^{4+}) metal ions on the phosphorylated Si substrate was about -7 V at the scan speed of 1 μm/s, but about -13 V for divalent(Ca^{2+}, Mg^{2+}) metal ions. That is, since the surface charge of divalent metal phosphate monolayer is neutral, this monolayer has a certain potential energy barrier that is a threshold energy required for the anodic oxidation with electrons transferred from tip to surface. Figure 5 shows the protruded and etched oxide patterns on Zr^{2+} phosphate monolayer by AFM anodization. The average full width at half maximum(FWHM) and the protruded oxide height displayed through AFM topography profile analysis are about 78 nm and 2 nm, respectively, in Figure 5(a) and about 50 nm and 0.8 nm, respectively, in Figure 5(b). Then the protruded oxide patterns were selectively etched with an aqueous solution of 0.25 wt% hydrofluoric acid while the unpatterned region was protected from etching by the Zr^{2+} phosphate SAM. Although general SAMs are gradually degraded in HF solution, the Zr^{2+} phosphate monolayer on Si substrate endured for at least for 3 min in 0.25 wt% HF solution. The etch depth and width of fine grooves were about 1.5 nm and 86 nm in Figure 5(c), and about 0.6 nm and 56 nm in Figure 5(d), respectively. Positively charged tetravalent metal phosphate monolayers effectively accept electrons from tip to substrate so that the anodization occurred at even higher speed and lower bias voltage.

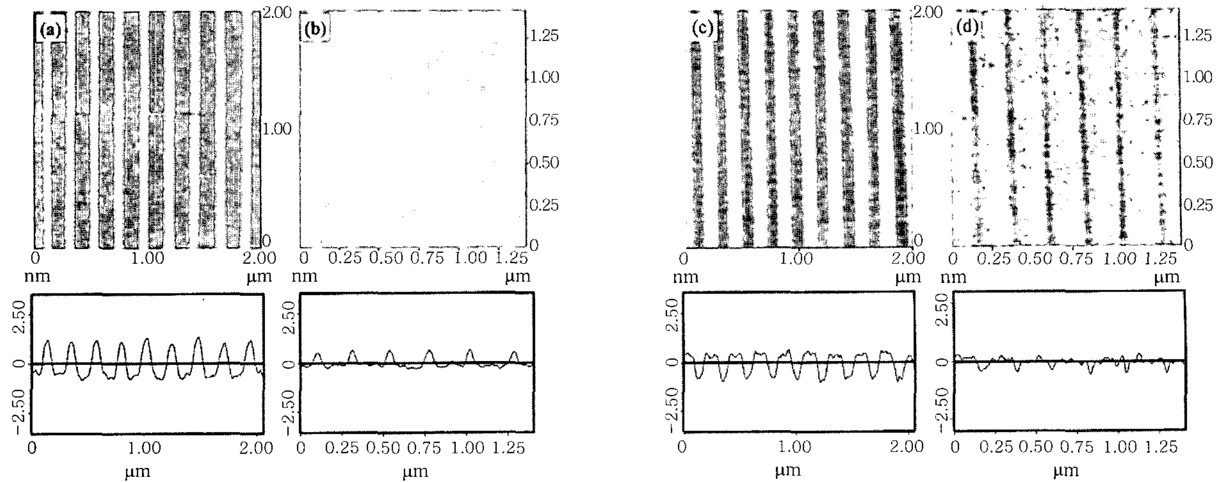

Figure 5. AFM topographic image of a line oxide patterned by AFM anodization (a) at –15 V tip bias and a scan speed of 100 μm/s and (b) at –16 V tip bias and a scan speed of 500 μm/s. (c) The fine grooves after etching the oxide patterns of (a) in an aqueous solution of 0.25 wt% HF for 2 min, and (d) after etching the patterns of (b).

AFM Anodization Lithography on Langmuir-Blodgett (LB) Films : Several research groups reported that the resist films could be adapted to the AFM anodization lithography to fabricate the high-resolution patterns. Pattern with tens of nanometer line-width were easily obtained when an appropriate resist was selected. We used the easily acquirable Langmuir-Blodgett(LB) film of palmitic acid and hexadecylamine in order to elucidate the mechanism of AFM anodization process on an organic resist layer. A series of AFM images containing the lithographic stages at various bias voltages ranging from 4.00 to 8.00 V are shown in Figure 6. In the case of 4.00 V bias voltage in Figure 6(a), no visible change of surface topography is observed. However, there is a feeble grooved pattern at 5.00 V, which indicates the starting voltage of the degradation process. As the applied voltage increases, the degradation patterns are distinctively observed up to 5.85 V. When the bias voltage reached 6.00 V, the growth of oxide started to be observed at the bottom of the grooved pattern. At 8.00 V, the protruded oxide pattern was sufficiently grown with 1.1±0.5 nm height and 101±3 nm width. From the results, we suggested a two-step mechanism for the AFM anodization lithography on an organic resist layer. The first step is degradation of the organic resist and the next step is the formation of the silicon oxide due to the anodization reaction.

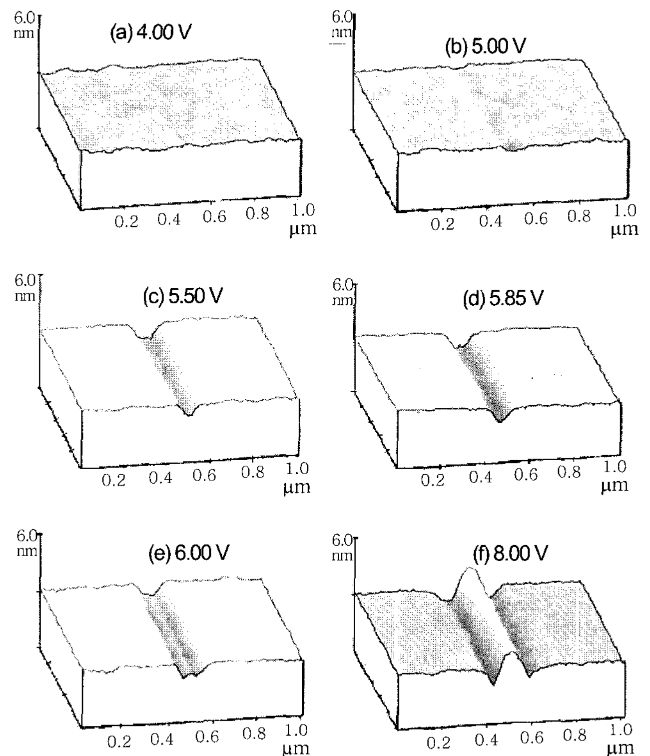

Figure 6. Lithographic pattern at constant lithographic speed at the specified voltage: (a) 4.00 V, (b) 5.00 V, (c) 5.50 V, (d) 5.85 V, (e) 6.00 V, and (f) 8.00 V.

Figure 7(a) shows the AFM images patterned at 5.50 V and tip speed of 1.0 μm/s. The degradation pattern with 202±5 nm of line-width and 0.7±0.3 nm of degradation depth is specified by difference between B and C points. The stripped substrate does not have the pattern of degradation but the protruded pattern with 212±4 nm of line-width and 0.8±0.3 nm of line-height as revealed in Figure 7(b). The complete stripping of the resist was confirmed by the topographical change of the landmark from 1.2±0.1 nm of vertical difference between B and D in

Figure 7(a) to 3.3±0.1 nm in Figure 7(b).

Among the several factors affecting AFM anodization lithography on an organic resist layer, the polarity change in the bias potential applied between the tip and the surface was investigated on palmitic acid LB film. In Figure 8(a), lithographic result obtained at −10 V of tip bias(tip negative; the normal polarity for AFM anodization lithography) shows the protruded pattern with 1.5±0.1 nm of height and 80±10 nm of width. The result acquired at 10 V of tip bias(tip positive), however, showed a grooved pattern with 2±0.2 nm of height and 80±10 nm of width as shown in Figure 8(b). The positive bias to the tip selectively removed the palmitic acid molecules and produced the negative pattern on the LB film. Two possible mechanisms were suggested for the lithographic process under positive tip bias. (i) Kolbe reaction and (ii) gradual degradation of resist films under strong electric field up to 10^7 V/cm. In Kolbe reaction, the palmitic acid should be dissociated via the following reaction.[46]

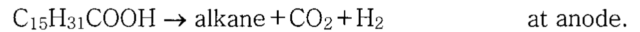

$$C_{15}H_{31}COOH \rightarrow \text{alkane} + CO_2 + H_2 \quad \text{at anode.}$$

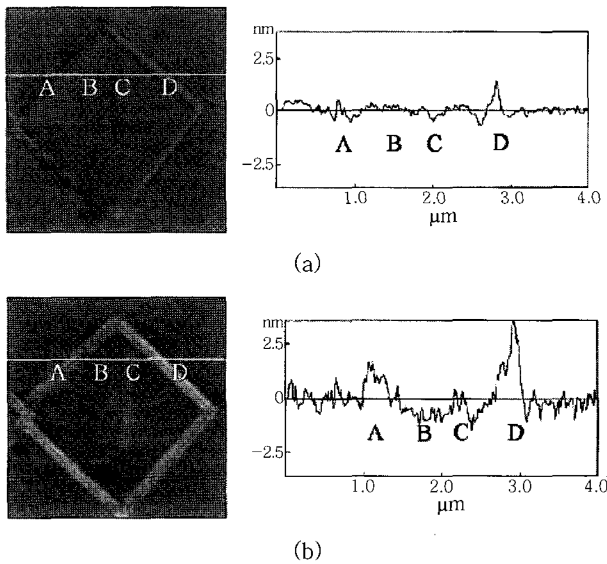

Figure 7. Topological views and cross sectional views of the patterned surface at 5.50 V bias voltage: (a) before stripping a resist film and (b) after stripping a resist film.

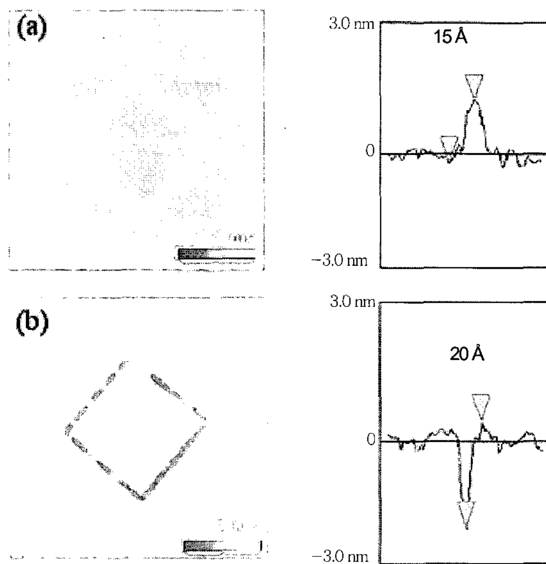

Figure 8. Lithographic pattern obtained at (a) −10 V and (b) 10 V with section analysis.

In the second case a degradation of the resist should be dependent upon the bias magnitude. To confirm the mechanism, the depth of the groove was measured while the bias was gradually increased from 5 V, starting lithographic voltage, to 10 V. It was found that the depth of a groove was gradually deepened as increasing the bias. This result may support the second mechanism rather than the first mechanism via Kolbe reaction.

AFM Anodization Lithography on Polymer Films : Besides the advantages of other organic resists for scanning probe lithography(SPL), polymer resists provide an attractive option because polymers can be easily deposited on a substrate and are well characterized from use in photolithography or e−beam lithography. Moreover, soft polymer surface minimizes the tip wear and therefore enables the patterning to be achieved at high speeds. The electron beam exposure makes bonds in polymer resist cleaved(positive resist) or crosslinked(negative resist). For positive resists the irradiated areas could dissolve once immersing in a developer. The resist pattern can then be transferred to the substrate using selective chemical etching or dry etching For example, SAL601, a chemically amplified resist, was patterned using the tip−induced electron exposure.[47] During electron beam exposure, an acid is generated in the resist which causes cross−linking during SPL exposure or during a subsequent post exposure bake(PEB) step. Even though SPL emits low energy electrons, the patterns were successfully produced due to the polymer's great sensitivity to the electrons.

To investigate the characteristics of AFM anodization lithography on a polymer film, we synthesized a methacrylate−based polymer composed of BPMA(1,3−bis(trimethylsilyl)isopropyl methacrylate), TFMA(tetra−hydrofurfuryl methacrylate) and MAA(methacrylic acid). The polymer is suitable for both ArF and AFM lithography. The spin−coated polymer was thermally stable up to 140 ℃ and was suitably resistant to the HF etching solution.

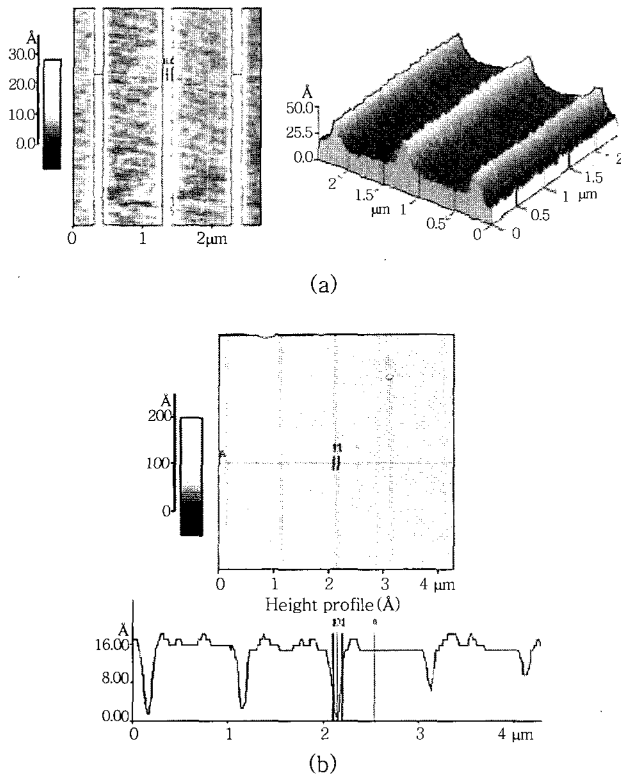

Figure 9. Topographic AFM images of (a) the protruded lines with 80 nm linewidth and 28 Å line height and (b) the etched Si grooves with 90 nm width and 15 Å depth.

Figure 9(a) shows the protruded lines with about 80 nm linewidth by AFM anodization lithography on spin-coated methacrylate-based polymer film. The fine pattern was obtained at -14～-15 V bias and a scan rate of 10 µm/s. The protruding patterns were etched under the optimal HF concentration of 0.33% HF and dipping time of 40 sec, resulted in fine grooves with 90 nm width as shown in Figure 9(b). The degraded region by AFM anodization became an etching window while the surrounding area was blocked from etching by the poly(BPMA-MAA-TFMA) resist film.

Summary

Several representative developments were introduced for anodic oxidation via AFM on organic resist layers of SAMs, LB films, polymers based on our works. The key to achieving high spatial precision and high speed is to select a sensitive organic resist for the electron exposure. In this view point, various resists were explored to investigate the exact mechanism of anodic oxidation on organic resist layers as well as their ability to accept tip-emitted electrons. The organic resist layers should be selectively resistant in dry or wet etching process to realize high resolution. More study, however, should be investigated for AFM-based anodization lithography to make it a generic method for nanometer scale fabrication process with high throughput. Use of organic resist layers will provide broad applications on AFM-based lithography due to their photonic and electronic sensitivity, various chemical functionalities, resistance, and mechanical softness, etc. Our studies shall serve as a useful guide for future nanoelectronics and biotechnology.

Acknowledgements. This work was supported by the National Program for Tera-Level Nanodevices of the Ministry of Science and Technology as on of the 21 Century Frontier Programs.

References

1. G. Binnig, H. Rohrer, C. Gerber, and E. Weibel, *Phys. Rev. Lett.*, **49**, 57 (1982).
2. G. Binnig, C. F. Quate, and Ch. Gerber, *Phys. Rev. Lett.*, **56**, 930 (1986).
3. G. Marsh, *Materialstoday*, **6**, 28 (2003).
4. P. Gould, *Materialstoday*, **6**, 34 (2003).
5. D. Wouters and U. S. Schubert, *Angew. Chem. Int. Ed.*, **43**, 2480 (2004).
6. G. Y. Liu, S. Xu, and Y. Qian, *Acc. Chem. Res.*, **33**, 457 (2000).
7. R. M. Nyffenegger and R. M. Penner, *Chem. Rev.*, **97**, 1195 (1997)
8. B. D. Gates, Q. Xu, M. Stewart, D. Ryan, C. G. Willson, and G. M. Whitesides, *Chem. Rev.*, **105**, 1171 (2005).
9. S. H. Lee and H. Lee, *Encyclopedia of Nanoscience and Nanotechnology*, Marcel Dekker, Inc., New York, p109 (2004).
10. D. M. Eigler and D. K. Schweizer, *Nature*, **344**, 524 (1990).
11. I-W. Lyo and Ph. Avouris, *Science*, **253**, 173 (1991).
12. R. D. Piner, J. Zhu, F. Xu, S. Hong, and C. A. Mirkin, *Science*, **283**, 661 (1999).
13. S. L. Brandow, W. J. Dressick, C. S. Dulcey, T. S. Koloski, L. M. Shirey, J. Schmidt, and J. M. Calvert, *J. Vac. Sci. Technol. B*, **15**, 1818 (1997).
14. M. Versen, B. Klehn, U. Kunze, D. Reuter, and A. D. Wieck, *Ultramicroscopy*, **82**, 159 (2000).
15. E. Garfunkel, G. Rudd, D. Novak, S. Wang, G. Ebert, M. Greenblatt, T. Gustafsson, and S. H. Garofalini, *Science*, **246**, 99 (1989).
16. P. Radojkovic, M. Schwartzkopff, T. Gabriel, and E. Hartmann, *Appl. Phys. A*, **66**, S701 (1998).
17. P. E. Sheehan, L. J. Whitman, P. K. William, and A. N.

Brent, *Appl. Phys. Lett.,* **85**, 1589 (2004).
18. S. W. Lee, B. J. Park, G. Y. Yeom, and H. Lee, *Nano−technology,* **16**, 3137 (2005).
19. J. A. Dagata, J. Schneir, H. H. Haray, C. J. Evans, M. T. Postek, and J. Bennet, *Appl. Phys. Lett.,* **58**, 2001 (1990).
20. R. M. Silver, E. E. Ehrichs, and A. L. de Lozanne, *Appl. Phys. Lett.,* **51**, 247 (1987).
21. M. Baba and S. Matsui, *Jpn. J. Appl. Phys.,* **29**, 2854 (1990)
22. S. L. Konsek, R. J. N. Coope, T. P. Pearsall, and T. Tiedje, *Appl. Phys. Lett.,* **70**, 1846 (1997).
23. S. Xu and G. Y. Liu, *Langmuir,* **13**, 127 (1997).
24. J. F. Liu, S. Cruchon−Dupeyrat, J. C. Garmo, J. Frommer, and G. Y. Liu, *Nano Lett.,* **2**, 937 (2002).
25. J. Zhao and K. Uosaki, *Nano Lett.,* **2**, 137 (2002).
26. A. E. Gordon, R. T. Fayfield, D. D. Litfin, and T. K. Higman, *J. Vac. Sci. Technol. B,* **13**, 2805 (1995).
27. H. Sugimura and N. Nakagiri, *J. Vac. Sci. Technol. A,* **14**, 1223 (1996).
28. D. Stievenard, P. A. Fontaine, and E. Dubois, *Appl. Phys. Lett.,* **70**, 3272 (1997).
29. P. Avouris, T. Hertel, and R. Martel, *Appl. Phys. Lett.,* **71**, 285 (1997).
30. J. Kim, Y. Oh, H. Lee, Y. Shin, and S. Park, *Jpn. J. Appl. Phys.,* **37**, 324 (1998).
31. B. Legrand and D. Stievenard, *Appl. Phys. Lett.,* **74**, 4049 (1999).
32. E. S. Snow, P. M. Campbell, and F. K. Perkins, *Appl. Phys. Lett.,* **75**, 1476 (1999).
33. W. Lee, Y. Oh, E. R. Kim, and H. Lee, *Synthetic Metals,* **117**, 305 (2001).
34. S. J. Ahn, Y. K. Jang, and H. Lee, *Appl. Phys. Lett.,* **80**, 2592 (2002).
35. H. Lee, S. A. Kim, S. J. Ahn, and H. Lee, *Appl. Phys. Lett.,* **81**, 138 (2002).
36. W. Lee, E. R. Kim, and H. Lee, *Langmuir,* **18**, 8375 (2002).
37. M. S. Son, E. R. Kim, and H. Lee, *J. Korean Phys. Soc.,* **41**, 949 (2002).
38. S. M. Kim and H. Lee, *J. Vac. Sci. Technol. B,* **21**, 2398 (2003).
39. S. J. Bae, C. Han, M. S. Kim, C. C. Chung, and H. Lee, *Nanotechnology,* **16**, 2082 (2005).
40. W. Lee, H. Lee, and M. S. Chun, *Langmuir,* **21**, 8839 (2005).
41. M. Tello and R. Garcia, *Appl. Phys. Lett.,* **79**, 424 (2001).
42. A. Ulman, *An introduction to ultrathin organic films from Langmuir−Blodgett to self−assembly,* Academic Press, San Diego, 1991.
43. H. J. Lee, H. Y. Park, S. Y. Koo, and H. Lee, *Mat. Res. Soc. Proc.,* **739**, 199 (2003).
44. Q. Li, J. Zheng, and Z. Liu, *Langmuir,* **19**, 166 (2003).
45. J. N. Israelachvili, *Intermolecular and Surface Forces: With Applications to Colloidal and Biological Systems,* 2nd ed., Academic Press, New York, 1992.
46. H. Kolbe, *Ann.,* **69**, 257 (1849).
47. K. Wilder, B. Singh, D. F. Kyser, and C. F. Quate, *J. Vac. Sci. Technol. B,* **16**, 6 (1998).